Turbocharging Ambient Backscatter Communication

Aaron N. Parks[†], Angli Liu[†], Shyamnath Gollakota, Joshua R. Smith
University of Washington
{anparks, anglil, gshyam, jrsjrs}@uw.edu
[†]Co-primary Student Authors

ABSTRACT

Communication primitives such as coding and multiple antenna processing have provided significant benefits for traditional wireless systems. Existing designs, however, consume significant power and computational resources, and hence cannot be run on low complexity, power constrained backscatter devices. This paper makes two main contributions: (1) we introduce the first multi-antenna cancellation design that operates on backscatter devices while retaining a small form factor and power footprint, (2) we introduce a novel coding mechanism that enables long range communication as well as concurrent transmissions and can be decoded on backscatter devices. We build hardware prototypes of the above designs that can be powered solely using harvested energy from TV and solar sources. The results show that our designs provide benefits for both RFID and ambient backscatter systems: they enable RFID tags to communicate directly with each other at distances of tens of meters and through multiple walls. They also increase the communication rate and range achieved by ambient backscatter systems by 100X and 40X respectively. We believe that this paper represents a substantial leap in the capabilities of backscatter communication.

CATEGORIES AND SUBJECT DESCRIPTORS

C.2.1 [**Network Architecture and Design**]: Wireless communication

KEYWORDS

Backscatter; Internet of Things; Energy harvesting; Wireless

1. INTRODUCTION

The last decade has seen significant advances in wireless communication — Wi-Fi systems today can achieve bit rates as high as 300 Mbps [2] and cellular networks can operate at ranges of tens of kilometers [3]. These impressive rate and range capabilities have been made possible by communication primitives such as coding mechanisms and multi-antenna processing. These techniques, however, are not suitable for battery-free devices such as RFID tags and ambient power harvesting sensors: Existing multi-antenna designs consume power on the order of a few Watts [14]; this is orders of magnitude more power than is available on harvesting devices [24]. Similarly, coding techniques that enhance communication range and enable concurrent transmissions (e.g., CDMA) consume substantial power and computational resources that limit their applicability to low-power devices.

SIGCOMM'14, August 17–22, 2014, Chicago, IL, USA.

http://dx.doi.org/10.1145/2619239.2626312.

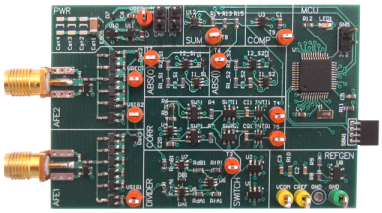

Figure 1—Our Prototype integrates both μmo and μcode in a single design. It can operate using both RFID and TV transmissions.

The key reason for this is that these techniques assume the ability to perform complex digital signal processing — multi-antenna processing requires estimating channel parameters and performing operations such as matrix inversion; coding techniques (e.g., CDMA) require performing computationally expensive correlation and synchronization. These methods are infeasible on battery-free devices as obtaining a digital representation of a signal requires power-intensive ADCs, and performing computationally expensive tasks is also expensive in terms of power consumption.

In this paper, we ask if it is possible to achieve the benefits of these communication primitives on battery-free devices. The intuition we leverage is as follows: since the power-intensive nature of these techniques is due to their use of ADCs and digital computation, if we instead perform computation in the analog domain we can achieve orders of magnitude reduction in the power consumption. Using this as our guiding principle, we design two communication primitives for backscatter communication: *μmo*, a multi-antenna receiver that is powered using harvested energy, and *μcode*, a low-power coding mechanism that enables large communication ranges and concurrent transmissions, and can be decoded using simple analog components on battery-free devices.

μmo. To understand our low-power multi-antenna design, consider the ambient backscatter [24] setting in Fig. 2 with two battery-free devices, Alice and Bob, where Bob communicates with Alice by backscattering the signals from the TV tower. Existing designs consider the TV transmissions to be noise, and hence achieve very low bit rates. Alice, however, can use multiple antennas to separate Bob's reflections from the direct TV signals, thus achieving significantly higher rates. The key challenge however is that conventional multi-antenna decoding hinges on estimating the amplitude and phase of the channel between the transmitters and the receive antennas. Since acquiring phase information is power-intensive, it is not available on backscatter devices [20]. This makes conventional multi-antenna decoding infeasible on backscatter devices.

To address this challenge, we present a multi-antenna technique that enables Alice's receiver to decode Bob's backscattered transmission without estimating the channel parameters. The intuition

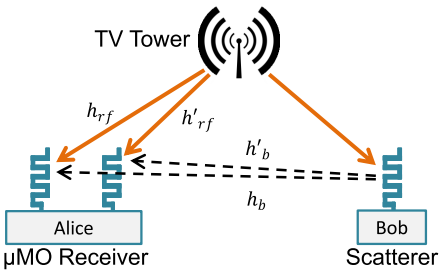

Figure 2—μmo Decoding. The two-antenna device, Alice, can decode Bob's backscattered information by separating the direct TV transmissions from the backscattered signals. μmo achieves this operation with neither channel estimation nor digital computation.

underlying our approach is best explained using an example. Let $s(t)$ be the signal from the TV tower and suppose Bob conveys '1' ('0') bit by reflecting (not reflecting) the TV signals. Alice now receives the following signals on its two antennas:

$$y_1(t) = h_{rf}s(t) + h_bBs(t)$$
$$y_2(t) = h'_{rf}s(t) + h'_bBs(t)$$

where h_{rf},h'_{rf} and h_b, h'_b are the channels from the TV tower and Bob to the two antennas on Alice, respectively. Further, B is 1 when Bob reflects the signals and is 0 otherwise.

μmo decodes the backscattered bits without estimating any channel parameters. Specifically, the receiver computes $\frac{y_1(t)}{y_2(t)}$ which is either $\frac{h_{rf}}{h'_{rf}}$ or $\frac{h_{rf}+h_b}{h'_{rf}+h'_b}$ depending on whether the backscattered bit is '0' or '1'. Thus, the receiver can decode the backscattered data without performing channel estimation. In §4 we explore the above idea further and describe how the above operation can be performed using simple analog components, without requiring digital computation.

μcode. Coding mechanisms (e.g., CDMA) have been used in conventional radios to significantly increase the range of communication and enable concurrent transmissions. These techniques use pseudorandom codes to encode information at the transmitter; the receiver synchronizes with the transmit signal and decodes the information by correlating with the pseudorandom codes. The challenge in using these designs is that the correlation and synchronization operations are computationally expensive and are difficult to perform on backscatter devices.

To address this problem, we introduce a low-power coding scheme for backscatter communication that does not require synchronization. Our intuition is that periodic signals such as sinusoidal waves can be detected without the need for synchronization; thus we design μcode to mimic a sine wave. Specifically, instead of using pseudorandom sequences, we use periodic sequences of alternating zeros and ones as the code. We show that such a design eliminates the need for synchronization operations at the receiver while providing large communication ranges. Further, the receiver can decode using only analog components, thus reducing its power consumption. Finally, we demonstrate that μcode can also enable multiple concurrent transmissions in a network of battery-free devices, without the need for synchronization between transmitters.

We build multiple hardware prototypes (one of which is shown in Fig. 1) that integrate both μmo and μcode in a single system. To demonstrate the benefits of our designs for backscatter communication, we build two different prototypes: the first prototype enables ambient backscatter communication using TV transmissions in the 539 MHz frequency range. The second prototype enables RFID tag-to-tag communication using RFID reader transmissions in the 915 MHz range. Note that tag-to-tag communication is a novel capability that is in contrast to conventional RFID systems, where the RFID tags communicate with the reader but not with each other. We run experiments in various line-of-sight and non-line-of-sight scenarios at various bit rates from 0.33 bps to 1 Mbps. Our experiments show the following:

- Our μmo prototype consumes 422 μW. In comparison, traditional Wi-Fi multi-antenna transceivers consume more than one Watt [14]. μcode, on the other hand, consumes about 8.9 μW. At an ambient illuminance of 330 lux, we could continuously power μmo and μcode using a photovoltaic array with an area of 8.28 square inches and 0.17 square inches, respectively. By using duty-cycling to reduce average power requirements, the prototypes can also operate on energy from ambient TV signals.
- μmo increases ambient backscatter's data rate by 100X from 10 kbps to 1 Mbps by providing multi-antenna cancellation; μcode increases ambient backscatter's range by a factor of 40X from two feet to more than 80 feet through coding gain. This significantly expands the range of applications where ambient backscatter can be used.
- μcode enables RFID tags to communicate with each other at distances of more than 80 feet and between different rooms that are separated by up to three walls. This reduces the need for deploying RFID readers throughout the environment, which is a substantial value proposition.

Contributions: We make the following contributions:

- We present μmo, the first multi-antenna interference cancellation design that can operate on backscatter devices. To do this, we introduce a multi-antenna decoding mechanism that does not require channel estimation and can be achieved using simple analog components.
- We present μcode, a novel coding mechanism that can significantly increase the backscatter communication range and can be decoded on backscatter devices. Using μcode we enable concurrent transmissions in a network of battery-free devices.
- Finally, we build hardware prototypes for μmo and μcode and show that they significantly expand the capabilities of backscatter systems. Specifically, we provide orders of magnitude increase in the communication rate and range of ambient backscatter. We also enable RFID tag-to-tag communication at long ranges and in through-the-wall scenarios, which was previously not possible.

2. Related Work

Our work is related to prior work in both conventional radio communication and backscatter communication:

(a) Radio Communication: There has been significant interest in multi-antenna systems and coding mechanisms to improve the performance of traditional Wi-Fi and cellular systems [36, 12, 40] . These techniques, however, require computationally expensive digital signal processing and power-consuming analog components (e.g., ADCs). In contrast, our work eliminates the need for ADCs and digital signal processing, and achieves multi-antenna cancellation and coding gains on backscatter devices.

Our work is also related to low-power MIMO radio designs [38, 8, 34, 18, 22]. These designs increase the energy efficiency of MIMO by optimizing the decoding algorithms [8, 34] and the processor designs [18, 22]. They operate in the digital domain, and thus require power-consuming ADCs. This makes them inapplicable to backscatter devices.

Prior work on low-power spread spectrum transceivers [25, 19, 26, 9, 11] has attempted to reduce the power consumption of digital operations such as synchronization and correlation. These systems

use traditional radio architectures with power-consuming RF oscillators and ADCs that are not available on a backscatter device. In contrast, we are the first to design and implement CDMA-like codes on backscatter devices that do not require digital signal processing, and hence consume orders of magnitude less power.

Finally, our work is related to work in the area of analog signal processing [30, 32, 33]. Before the advent of digital processors, wireless communication was performed on analog circuits. Ultra-wide band communication and radar systems still use analog correlators to reduce the cost of hardware components [30, 31, 21]. We build on this foundational work but differ from it in that we are the first to apply this principle to achieve multi-antenna cancellation and channel coding benefits on backscatter devices. Further, we introduce algorithms, techniques, and circuits to achieve this goal.

(b) Backscatter Systems: There has been recent interest in improving the performance of backscatter communication [41, 6]. Recent work on ambient backscatter [24] enabled devices to communicate by backscattering existing RF signals like TV transmissions. However, current designs are limited to communication ranges of two feet and communication rates of 10 kbps. Similarly, work on RFID tag-to-tag communication [28] enabled two RFID tags to communicate with each other in the presence of an RFID reader at distances of up to 25 mm. Our work significantly improves the capabilities of these systems. Specifically, using μmo and μcode, we demonstrate ambient backscatter communication at distances greater than 80 feet and communication rates of 1 Mbps using TV signals. We also show the feasibility of RFID tag-to-tag communication at distances of tens of meters, even when multiple walls separate the tags.

Recent work on MIMO RFID systems [15, 35, 23, 29, 4, 10] leverage multi-antenna capabilities to improve the throughput and reliability of RFID communication. These systems focus on the communication between a multi-antenna reader and a single-antenna backscatter device, and thus the computationally intensive and power-consuming MIMO operations are performed on the powered reader. Recent information theoretic work [13, 16, 17, 7] characterizes the diversity gains achieved by using multiple antennas on backscatter devices. In contrast, we introduce μmo, a novel multi-antenna technique that can decode the backscattered information by cancelling the interference from ambient signals. We believe that μmo is the first design and implementation of multi-antenna cancellation on a backscatter device.

Finally, prior work has proposed to use CDMA to address the problem of collisions in RFID networks [37, 5, 27, 39]. In these systems a code is assigned to each backscatter device, and the powered RFID reader correlates with the code to decode the transmitted data even in the face of collisions. These systems are however designed for uplink communication from the backscatter device to an RFID reader, and do not enable decoding on a low power backscattering device. In contrast, we present μcode, the first coding mechanism that provides the benefits of CDMA and can be decoded on a backscattering device; we also show that μcode can enable concurrent transmissions in a network of battery-free devices.

3. OUR DESIGN PRINCIPLE

Our goal is to design primitives that enhance wireless communication capabilities on battery-free devices. The key challenge in achieving this is that wireless primitives such as multi-antenna and coding use digital signal processing that requires power-intensive ADCs and computationally expensive digital operations. To address this challenge, we use the following guiding principle: eliminate the need for digital processing by enabling computation in the analog domain. Such an approach, as we show in the rest of the paper, can provide an order of magnitude reduction in the power consumption of these communication primitives.

In the rest of this paper, we describe μmo, our low-power multi-antenna backscatter receiver and show how it can improve the communication rate of ambient backscatter. We then describe μcode, our low-power coding technique that is achieved using simple analog components, and show how it can be used to increase the communication range of backscatter systems. Finally, we show that our designs can be used to enable concurrent transmissions in a network of battery-free devices, without the need for synchronization.

4. μMO

We first motivate the need for multi-antenna cancellation in ambient backscatter systems and then describe the challenges in achieving μmo. We then describe our receiver design that addresses these challenges.

4.1 Motivation and Challenges

Multi-antenna designs are known to provide communication rate gains that are linear with the number of antennas at the receiver; linear improvements, however, might not be a compelling motivation for low-power designs. So we demonstrate next that multi-antenna cancellation can provide orders of magnitude communication rate improvements for ambient backscatter systems [24]. Ambient backscatter enables two battery-free devices, Alice and Bob, to communicate with each other by backscattering ambient signals in the environment (e.g., TV transmissions). This is in contrast to traditional backscatter systems (e.g., RFID), where the communication is between a battery-free tag and a powered RFID reader and works only in the presence of an RFID reader.

At a high level, the backscattering device encodes a '1' bit by reflecting the incident ambient signals and a '0' bit by absorbing them. The challenge in achieving this is that the ambient signals (e.g., TV) carry information and hence change significantly with time. Prior designs [24] average out the fast-changing TV transmissions to decode the backscattered signals. Averaging removes the variations inherent to the ambient signals, thus allowing the receiver to decode the backscattered signals.

The key issue with averaging, however, is that the backscattering device can transmit information only at a rate that is lower than that of the averaging. Specifically, if the receiver averages the TV transmissions over 100 ms, then the backscattering device can only transmit at a maximum rate of 10 bps. Similarly, if the receiver averages transmissions over one millisecond, then the maximum backscatter rate is 1 kbps. Since averaging must be done over a significant period of time to smooth out the variation in the TV transmissions, averaging does not allow rates much higher than 10 kbps [24]. Intuitively, this is because existing designs decode the backscattered information by considering the ambient signals (e.g., TV) as noise. Since the strength of the TV signal is significantly higher than that of the backscattering signal, the channel has a very low SNR and hence achieves a very low communication rate.

Using multiple antennas, one can eliminate interference from TV signals, and hence provide orders of magnitude higher bit rates.[1] To see this, consider the 2-antenna receiver in Fig. 2. Suppose $s(t)$ is the signal transmitted by an ambient RF source (e.g., TV tower) and that the backscattering device conveys a one bit by reflecting the TV signals and a zero bit by not reflecting them. Now, the receiver

[1]Note that we aim to use multiple antennas for interference cancellation rather than leverage them for antenna diversity. This is because while antenna diversity can reduce the amount of averaging required (e.g., halve it with a two antenna system) it does not eliminate the interference from TV signals.

receives the following signals on its two antennas.

$$y_1(t) = h_{rf}s(t) + h_bB(t)s(t)$$
$$y_2(t) = h'_{rf}s(t) + h'_bB(t)s(t)$$

where h_{rf}, h'_{rf} and h_b, h'_b are the channels from the RF source (TV tower) and the backscattering device respectively. In principle, if the receiver can estimate the channel parameters, h_{rf}, h'_{rf} and h_b, h'_b, it would have two equations in two unknowns, $s(t)$ and $B(t)$; thus it can decode the backscattered information, $B(t)$ by performing a matrix inversion operation on the received signals.

Achieving the above operations on a backscatter device, however, is challenging for two main reasons:

- Channel estimation requires computing both the amplitude and phase on the receiver. Estimating the phase information requires the use of a local oscillator; an oscillator must operate at the carrier frequency, therefore consuming more power than is available. Thus backscatter devices do not have the phase information required to perform channel estimation.
- Decoding the backscattered signal is done by performing matrix inversion on a digital representation of the received signal. Digitizing the analog signals requires an 8-12 bit resolution ADC that operates at the communication rate; this again consumes more power than is available on a backscatter device.

4.2 μmo Decoding Algorithm

μmo can decode backscatter signals with neither phase information nor ADCs. In this section, we describe our algorithm to decode the backscatter signal without estimating the channel parameters. In the next section, we show how the algorithm can be achieved using only analog computation.

Our intuition is as follows: Since backscattering creates an additional reflection to the receiver, the effect of backscatter is to change the channel at the receiver. Further, since the reflected signal propagates by different distances to the two antennas at the receiver, the channel changes created on the two antennas are different. Thus, by comparing the relative channel changes across the two antennas, we can identify the bits transmitted by the backscattering device.

More formally, μmo first computes the amplitude of the received signal on the two antennas to get:

$$|y_1(t)| = |h_{rf}s(t) + h_bB(t)s(t)|$$
$$|y_2(t)| = |h'_{rf}s(t) + h'_bB(t)s(t)|$$

where $|a|$ represents the magnitude of a. Dividing the above equations, we have the following fraction:

$$\frac{|y_1(t)|}{|y_2(t)|} = \frac{|h_{rf} + h_bB(t)|}{|h'_{rf} + h'_bB(t)|}$$

Note that the above fraction is independent of the TV signal $s(t)$, and hence is not affected by the envelope fluctuations inherent in TV transmissions. Now, since the backscattered bits $B(t)$ are either '1' or '0', the above fraction gives us either $\frac{|h_{rf}|}{|h'_{rf}|}$ or $\frac{|h_{rf}+h_b|}{h'_{rf}+h'_b}$. Thus, the above fraction computation results in two different levels depending on whether the backscattered bit is a zero or a one.

To see the above computation in practice, we use a backscatter device to transmit an alternating sequence of zeros and ones at a rate of 1 *kbps*, by backscattering 539 MHz TV transmissions. We use a USRP equipped with two antennas separated by half a wavelength to capture the received digital signals from a distance of 3 feet. Fig. 3 (a) and (b) plot the received signal on each of the receive antennas. The figures show that it is difficult to see the backscattered signal in the presence of the TV transmissions. Fig. 3 (c) plots the result of dividing the received signals on the two antennas. The plot shows that now the alternating sequence of backscattered bits is visible, allowing the receiver to decode.

We note the following key points:

- The above computation does not guarantee that the output corresponding to a '1' bit is always greater than that corresponding to a '0' bit. In particular, the ratio of the amplitudes on the two antennas depends on h_{rf}, h'_{rf}, h_b, and h'_b, which change with device positions. To address this ambiguity, the receiver uses the preamble bits sent by the transmitter to extract the mapping.
- We note that while noise increases the BER at the receiver, it does not affect the correctness of the above equations. Further, in the above discussion, we assume that the channel is determined by a single channel parameter; since backscattering devices do not use oscillators, they are not frequency selective in their behavior. Thus it is reasonable to approximate the channel at the backscatter device as a single parameter.

4.3 μmo's Hardware Design

Next, we describe how μmo achieves the above algorithm using only simple analog components, thus eliminating the need for power-consuming components such as ADCs.

The μmo receiver has three main stages: 1) an envelope detection circuit that computes the amplitude of the received signal on each antenna, 2) an analog circuit that imitates the division operation to find the ratio of the signal envelopes received by the two antennas, and 3) a thresholding circuit that extracts the backscattered bits. We explain each of these components in detail.

1) Envelope Detection Circuit. The role of the envelope detector is to track the envelope of the received signal, while eliminating the carrier frequency (539 MHz in case of TV transmissions). The circuit in the figure uses passive components such as resistors, capacitors, and diodes and hence is ultra-low power in nature. The operating principle behind an envelope detector is similar to that used in an RFID tag: diodes act as switches that allow current to flow in the forward direction but not the reverse, capacitors are charge-storage elements and resistors regulate current flow. By choosing the appropriate values for these analog components, we can remove the carrier frequency (e.g., 539 MHz) and leave only the amplitude of the signal. As shown in Fig. 4, μmo performs the envelope detection computation on both the receiver antennas.

2) Divider Circuit. The next step is to divide the amplitudes received on the two antennas. Performing division in a low-power manner is not straightforward, particularly since analog dividers are not a commonly implemented primitive on low power devices. μmo employs simple logarithmic identities to split the division operation into several easily implemented steps, using the following mathematical trick:

$$\frac{a}{b} = e^{log(\frac{a}{b})} = e^{(log(a)-log(b))}$$

Specifically, to compute the quotient of two numbers a and b we can transform them into the logarithmic domain, subtract the two, and then exponentiate to get the result of the computation. μmo imitates the above math in the analog domain to perform division. In particular, μmo uses a log-amplifier on each of the receive signal envelopes to transform the signal amplitudes into the logarithmic domain. At a high level, log-amplifiers make use of the non-linear current-voltage (IV) relationship of a diode to convert a linear domain signal to a logarithmic representation. We then use an analog subtractor to compute the difference between the log-scale signal amplitudes on the two antennas. To get a true linear ratio signal, this difference would need to be transformed back into the linear

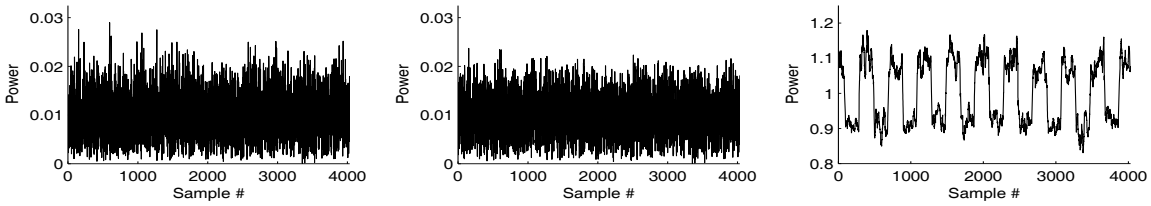

(a) Signal on the First Antenna (b) Signal on the Second Antenna (c) Result of μmo Division

Figure 3—μmo on actual signals. It is difficult to see the backscattered bits on the received signals at the two receiver antennas. Performing the division between the received signals on the two antennas, reveals the backscattered bits.

domain using an exponential amplifier (which would also make use of diode properties). However, because our next step is to perform a simple thresholding operation on the signal, we can make use of the fact that the log operation is monotonic and omit the exponential amplifier. Omitting this amplifier saves power by reducing the active component count, and does not impact the performance of the system as the simple thresholding operation is not impacted by the use of log domain signals.

3) Thresholding Circuit. The goal of this circuit is to distinguish between the two voltage levels at the output of the divider circuit. At a high level, the threshold circuit computes the mean of the two voltage levels, and outputs a one bit when the input is greater than the threshold and a zero bit otherwise. To compute this mean value, μmo uses an envelope detector as before. We use specific values for the resistors and the capacitors to compute the mean of the signal envelope. We then use a low-power comparator that outputs a one bit when the divider output is greater than the mean and a zero bit otherwise. As described in §4.2, the receiver uses a known preamble in the packet to flip the bits, if necessary, before decoding.

We note that the power consumption of analog components such as log-amplifiers and comparators depends on the bandwidth at which we would like our analog circuit to operate. The bandwidth of the analog circuit is defined as the maximum frequency that the circuit can process without severely attenuating the signals. In our case, we can set the analog bandwidth by selecting low-power amplifier and comparator components that can support a certain bandwidth. In our implementation, we build two different prototypes, one that operates at an analog bandwidth of 1 MHz and the other at an analog bandwidth of 1 kHz.

4.4 Putting Things Together

The discussion so far focuses on the physical layer of the μmo receiver. The backscatter transmitter uses the same physical layer as RFID systems to transmit messages with preambles and CRC checks. The transmitter can vary the transmitted bit duration and therefore the data rate. The receiver uses the low-power hardware design described above to decode messages, which are then validated by checking the CRC. The transmitter and the receiver use the same link layer mechanisms (including modulation and bit encoding) as prior backscatter systems. To conserve power, μmo's transmit hardware sends an alternating bit sequence long enough (8 bits in our implementation) to wake up the receiver's digital logic system, which then detects bit boundaries and performs framing.

5. μCODE

We first motivate the need for low-power coding designs for backscatter systems and then describe the challenges in achieving this goal. We then describe μcode's encoding and decoding algorithms that address these challenges. Finally, we present our decoder hardware design that uses only analog components.

5.1 Motivation and Challenges

RFID systems have seen a limited adoption, mainly due to limited read range and the resulting requirement for a dense deployment of RFID readers to communicate with RFID tags. If we can enable the RFID tags to communicate with each other at long ranges, we can significantly extend the effective read range by creating a multi-hop network across the RFID tags. Another backscatter technology that is currently limited by range is ambient backscatter [24], which eliminates the need for RFID readers by backscattering ubiquitous ambient signals like TV transmissions. While ambient backscatter does achieve tag-to-tag communication, the communication range of existing work is limited to two feet, which significantly limits its applicability. Thus, increasing the range of backscatter communication is essential to improving the viability of these systems.

Coding mechanisms such as CDMA can in principle be used to increase the communication range of backscatter systems. These techniques use a string of pseudorandom bits called chips to encode information bits. For example, the transmitter could represent a zero bit by the chip sequence '101110111' and a one bit by the chip sequence '111011011'. The 1s and 0s in the above sequences are the chips used by the transmitter to encode the information. To decode these information bits, the receiver correlates the received signal with the chip sequence patterns and converts correlation peaks to data bits. To increase the communication range, the transmitter-receiver pair uses longer chip sequences that effectively increase the signal-to-noise ratio and hence enable long-range communication. Decoding such transmissions on a backscatter device is challenging for two main reasons:

- The correlation operation required at the receiver is both computationally expensive and requires power-consuming ADCs that are not available on a backscatter device.
- More important, performing synchronization at the receiver is expensive. Synchronization requires correlating the received signal with a chip sequence for every offset of the received signal. This is not only computationally expensive but also consumes much more power than is available on our target device.

So any code that is to be decoded on a backscatter device should satisfy two main properties: 1) It should not require an ADC or digital signal processing operations, and 2) It should work without the need for synchronization.

5.2 μcode's Encoding and Decoding Algorithms

μcode can achieve coding gains on the backscatter device without requiring synchronization operations at the receiver. To understand μcode, we first explain the intuition using a simple sinusoidal wave; we then design the encoding and decoding algorithms to operate on the backscattered bits.

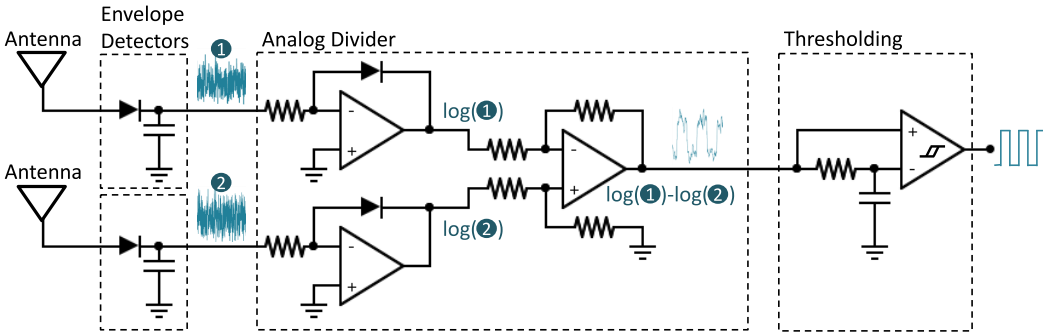

Figure 4—μmo hardware design. μmo performs the required computation using analog components. Specifically, μmo's hardware has three main components: an envelope detector that removes the carrier frequency (e.g., 539 MHz), an analog division circuit that divides the received signal on the two antennas, and finally a thresholding circuit that outputs the 0 and 1 bits.

Intuitively, instead of using a pseudorandom chip sequence, μcode uses a periodic signal to represent the information. To see why this works, consider a periodic sinusoidal signal transmitted at a specific frequency. If the receiver knows the frequency of the sinusoidal signal, it can detect the signal without any phase synchronization with the transmitter. Specifically, suppose the transmitter sends a sine wave, $sin(ft+\phi)$, with a frequency f and a phase offset ϕ. One can easily detect the above sine wave without phase synchronization by performing a dot product operation with the sine and cosine basis functions at the same frequency to compute the In-phase (I) and Quadrature phase (Q) components:

$$I = \sum_{t=0}^{T} sin(ft+\phi)sin(ft)\,\Delta t = \frac{1}{2}sin(\phi)$$

$$Q = \sum_{t=0}^{T} sin(ft+\phi)cos(ft)\,\Delta t = \frac{1}{2}cos(\phi)$$

where T is the duration over which the above dot product operation is computed.[2] Note that from the above equation,

$$|I|^2 + |Q|^2 = \frac{1}{2} \quad (1)$$

Since Eq. 1 is independent of the phase offset ϕ the receiver can detect the transmitted signal without the need for phase synchronization. Further, the receiver can increase its detection sensitivity by increasing the transmit signal duration, T. Thus, a simple periodic sine wave can be detected without requiring phase synchronization, and also provides a form of coding gain to increase reliability.

μcode's design builds on the above intuition. However, since our backscatter transmitter has only two states and therefore cannot transmit sine waves, it instead uses a periodic alternating sequence of zeros and ones. Specifically, it encodes the one bit by the chip sequence $101010\cdots10$ and the zero bit by the chip sequence $000000\cdots00$.

Our decoder imitates the I and the Q computation above to detect the alternating one-zero sequence, without the need for synchronization. Specifically, it computes the in-phase component (I) by a dot-product operation with the chip sequence $101010\cdots10$ and the quadrature-phase component (Q) by a dot-product operation with a 90 degree offset chip sequence. This is similar to using the sine and the cosine function in the previous scenario. Note that a 90 degree offset is effectively a time offset of half a chip duration. To detect the presence of the alternating sequence of zeros and ones, the receiver then computes $|I|+|Q|$. This works independent of synchronization due to the following lemma:

LEMMA 5.1. *If the transmitter continuously sends an alternating sequence of zero and one chips and the receiver computes in-phase (I) and quadrature-phase (Q) components over any duration of N chips, then* $|I|+|Q| = N$.

The above lemma states that $|I|+|Q|$ is constant, independent of receiver synchronization (see appendix for the proof). Thus the receiver can detect an alternating sequence of zeros and ones by computing $|I|+|Q|$ over any duration of N chips. To summarize:

μcode's Encoding Algorithm. The transmitter uses the following chip sequences to represent the zero and one information bits:

$$1010\cdots N\cdots10 \quad \textit{as bit } 1$$
$$0000\cdots N\cdots00 \quad \textit{as bit } 0$$

where the chips are transmitted at a rate of C.

μcode's Decoding Algorithm. The receiver computes $|I|+|Q|$ over a duration of $\frac{n}{3}$ chips. If the majority vote of three adjacent computations is greater than a threshold then the receiver outputs a 1, and a 0 otherwise. The threshold is computed by taking the average of the received signal over bits in the preamble at the beginning of the transmitted packet.

The transmitter can control both the chip rate C and the chip length N to achieve different bit rates. The chip rate determines the duration of each chip bit; a higher chip rate corresponds to smaller chip durations. Given a chip rate, longer chip lengths result in larger ranges since they increase the signal-to-noise ratio. We also show in §8 that by controlling these parameters, we can create orthogonal codes that do not require any synchronization and can enable multiple concurrent transmissions.

5.3 μcode Hardware Design

Next we describe how μcode achieves the above decoding algorithm in the analog domain, without the need for ADCs.

Specifically, as shown in Fig. 5, our receiver design has four main components: an envelope detector circuit, $|I|$ and $|Q|$ computation blocks, an addition circuit, and a thresholding circuit. The envelope detector circuit is the same as that described in §4 and is used to remove the carrier frequency (e.g., 539 MHz TV transmissions). We implement the addition operation with an analog adder circuit, and the thresholding circuit is similar to that used in §4.

[2] We replace the integration operation that is typically performed with summation, for ease of exposition.

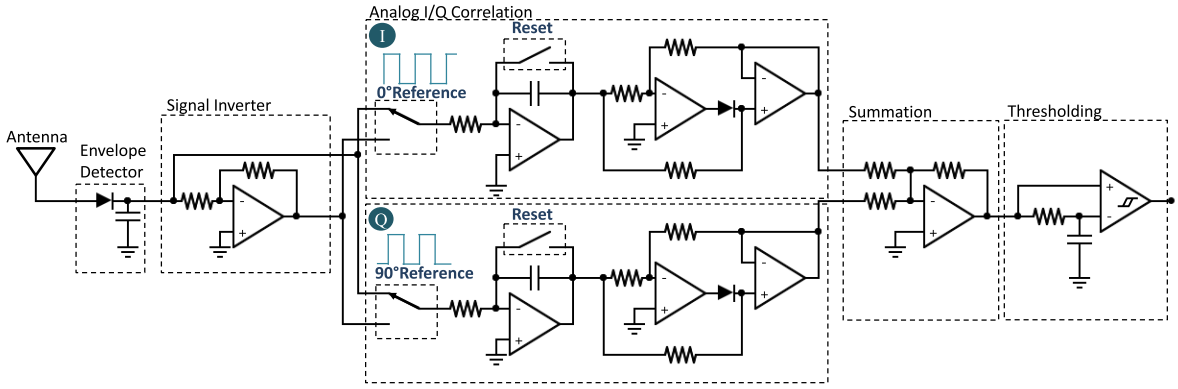

Figure 5—μcode hardware design. Our hardware design performs the decoding operations using analog components, without the need for ADCs. The hardware system has three main components: I/Q correlation circuits that compute |I| and |Q|, a summation circuit that computes |I| + |Q|, and finally a thresholding circuit that outputs 0 and 1 bits.

We focus the rest of this discussion on the $|I|$ and $|Q|$ computation circuits. Note that, functionally, both operations are similar to a dot product operation, multiplying two signals and accumulating the result over a time period (in our case the chip length N). The only difference between the $|I|$ and the $|Q|$ computations is that the chip sequence $10\cdots10$ is offset by 90 degrees for the $|Q|$ computation. Thus, we focus on the $|I|$ computation circuit. At a high level, we achieve the dot product operation (which is a multiply-accumulate operation) using three key components. First, we send the received signal through an analog inverter to generate the inverted version of the input signal. We then use an analog switch that toggles between the inverted and the non-inverted signal every T seconds, where T is the duration of a chip. This effectively achieves the multiplication operation with the chip sequence. Finally, we use an analog integrator to accumulate the output of this multiplication operation and compute $|I|$. The reset function in Fig. 5 is used to reset the circuit every chip sequence length duration to repeat the computation for every transmitted bit.

5.4 Enabling multiple transmissions using μcode

μcode can also be used to enable concurrent transmissions in the network without the need to deal with collisions or random access. Specifically, we show in the appendix that μcode satisfies the following property:

LEMMA 5.2. *A alternating zero-one chip sequence at a chip rate C is orthogonal to all chip sequences at a chip rate $2NC$ and chip length $2N$, where N is a positive integer. The orthogonality property holds independent of the synchronization between the codes.*

The above lemma implies that transmitters with codes that satisfy the above condition do not interfere with each other. Further, one can create codes with rates $C, 2C, 4C, 8C, \cdots$ such that every pair of chip sequences satisfy the above condition. By setting a particular value for C (say 100 Hz) and assigning different codes to different transmitter-receiver pairs, μcode can be used to enable concurrent interference-free transmissions. In §8 we evaluate μcode's ability to enable concurrent transmissions. One aspect of using different codes across transmitter-receiver pairs is the question of distributing these codes across the transmitters. Prior work on CDMA systems [27] has proposed a number of techniques including those that use collision-resistant hash functions to achieve this goal. In principle, we can combine μcode's design with these existing solutions; evaluating this, however, is not in the scope of this paper.

6. FURTHER DISCUSSION

We discuss the following aspects of our design:

(1) Bit Rate Adaptation. μmo and μcode each provide us with multiple bit rates; the transmitter-receiver pair can perform bit rate adaptation over all these rates to optimize the throughput and to account for channel fluctuations. We note that, for both systems, multiple bit rates can be achieved in hardware simply by changing timing parameters in the digital control logic. Our current prototype implementation allows us to pick different rates across μmo and μcode. Designing bit rate adaptation algorithms however is not in the scope of this paper.

(2) Interference with TV receivers. While the receiver designs in this paper increase the range and rate of backscatter communication, the backscattering operation at the transmitter is the same as in prior designs. Specifically, we do not change the strength of the backscattered signal at the transmitter over prior designs, and thus create no additional interference at TV receivers. Thus, similar to [24], our system creates interference at the TV receiver only when it is closer than eight inches from the TV antenna.

(3) Application to traditional RFID systems. This paper is focused on enabling communication between battery-free devices using backscatter. However, our designs can also be used to increase the downlink rate and range from an RFID reader to a tag. Current RFID reader-tag systems do not operate across different rooms and are limited to communication ranges that are comparatively smaller; our designs can in principle also provide between-room capabilities to traditional RFID reader to tag links.

7. PROTOTYPE IMPLEMENTATION

To evaluate the performance of μmo and μcode in practice, we designed and implemented the system on a printed circuit board as shown in Fig. 1. Our prototype integrates both the μmo and μcode designs on a single board. Fig. 6 shows a block diagram of our receiver prototype; it is a fully reconfigurable platform controlled by firmware executed on the low power MSP430 microcontroller. Both the μmo and μcode sections of the analog circuit are power-gated, i.e., they can be enabled or disabled easily to save power. Our prototype has the following features:

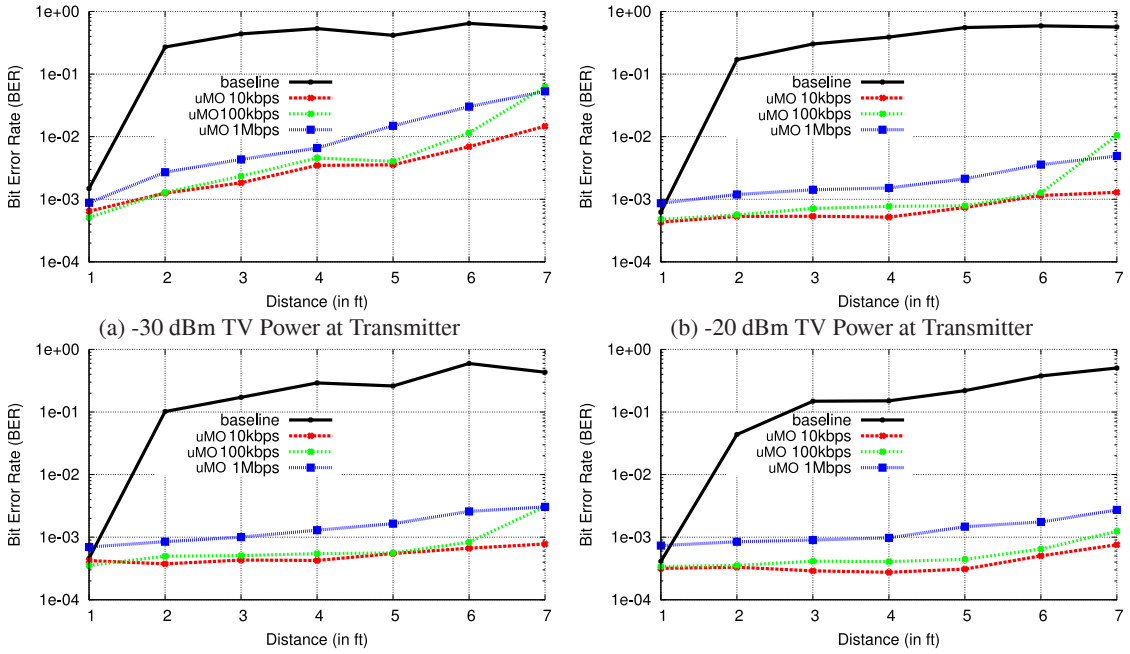

(a) -30 dBm TV Power at Transmitter

(b) -20 dBm TV Power at Transmitter

(c) -10 dBm TV Power at Transmitter

(d) 0 dBm TV Power at Transmitter

Figure 7—μmo BER versus Distance. The figure shows the bit error rate (BER) as a function of distance between the backscattering device and the receiver. The different plots correspond to different ambient RF power levels at the transmitter. The black solid line represents the baseline BER from existing ambient backscatter designs. The figure shows that μmo can enable data rates as high as 1 Mbps at distances between 4-7 feet. This translates to a 100X improvement in the data rates.

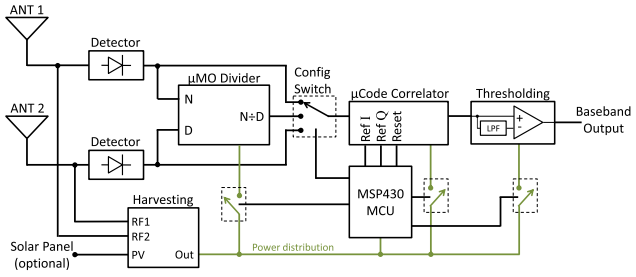

Figure 6—Block diagram of our receiver prototype

Table 1—Power consumption of Analog Signal Processing

	Max. Rate	Range	Rx Power
μcode	1 kbps	>80 ft	8.9 μW
μmo	1 Mbps	4 - 7 ft	422 μW

1) Flexible switching between μmo and μcode. We use an ultra-low-power configuration switch as shown in the figure to route signals between two modes of operation: μmo and μcode. When in μmo mode, the microcontroller directs the configuration switch to allow the output of the μmo divider to pass to the next decoding step. The μmo divider circuit is powered on, along with the thresholding circuit. When μmo is active, the μcode correlator is bypassed internally by forcing it into a perpetual reset state, which effectively disables any impact from the correlation circuit.

When in μcode mode, the switch is configured to route the signal from one of the two detectors to the correlator, allowing either of the two antennas to be selected as the signal source. The μcode correlator is powered on, along with the thresholding circuit. The microcontroller generates the correlator's reference I and Q chip sequences as well as a periodic reset pulse that clears the correlation result after every chip sequence duration. Note that in our experiments, we use only one receive antenna to evaluate μcode.

2) Trading analog bandwidth for lower power consumption. Every analog communication circuit has an constrained bandwidth, that is, there is a maximum baseband signal bandwidth that a receiver is capable of decoding. The analog bandwidth of a receiver is proportional to the maximum data rate that can be achieved using it. In our prototype, the analog bandwidth is determined by the capabilities of the operational amplifiers and other components we use to implement the analog processing. In general, higher bandwidth allows higher data rates but also increases power consumption.

We fabricate two prototypes: one that targets high-rate communication and consumes more power, and another that targets low-rate communication and consumes less power. Specifically, our high data rate prototype targets an analog bandwidth of 1 MHz. To achieve this we make use of the power-efficient TSV6390 operational amplifiers from ST Microelectronics in our signal processing circuits. For the final threshold comparison we use the NCS2200 comparator made by ON semiconductors. The low rate prototype, on the other hand, has an analog bandwidth of 1 kHz. To achieve this, we use the BU7265 operational amplifier from Rohm Semiconductor and the TS881 comparator from ST Microelectronics.

We use our high rate prototype to demonstrate μmo and our low rate prototype for μcode. Table 1 shows the power consumption of their analog signal processing, including all the analog components. The table shows that μmo consumes about 422 μW of power; this is in contrast to traditional Wi-Fi MIMO implementations [14] that use more than one Watt for a two-antenna receiver. The power consumption numbers for μcode are significantly lower at around 8.9 μW. We note that prior ambient backscatter designs use 0.54 μW of power but are significantly limited to less than two feet of communication range and 10 kbps of bit rates. The higher power consumption of our prototype, however, is not an issue since we use duty cycling to reduce the average power of these analog components, as described next. We also note that one can further reduce these power numbers by an order of magnitude by using application-specific integrated circuits (ASICs).

3) Energy Harvesting and Duty Cycling. Our prototype provides the ability to harvest energy from one or both of the following sources:

ambient TV energy, and solar power. In the case of an ambient RF energy harvesting supply, our prototype duty-cycles (periodically alternates between active and sleep states) to allow operation from such a low power source. With a typical TV harvesting power of 100 μW, our 1 MHz μmo device can operate 23% of the time, and the 1 kHz μcode system can operate 100% of the time.

In the case of a solar photovoltaic power supply, we consider the area requirement of a typical-efficiency solar array such that it can provide sufficient power for continuous operation of μmo and μcode circuits. To do this we measure the power output from an 2.75 by 1.38 inch thin film solar array (manufactured by PowerFilm Inc) in an environment with an illuminance of 330 lux. 330 lux is the minimal office and workplace illuminance specified by the Occupational Safety and Health Administration (OSHA) [1]. Given these measurements, μmo requires a 8.28 square inch solar array and μcode requires a 0.17 square inch solar array to continuously operate in our office environment.

8. EVALUATION

We first evaluate the performance of μmo in an ambient backscatter scenario. We then evaluate μcode for both ambient backscatter and RFID tag-to-tag communication in both line-of-sight and through-the-wall scenarios. Finally, we evaluate μcode's ability to enable multiple concurrent transmissions.

8.1 Evaluating μmo

We evaluate μmo in an ambient backscatter scenario where two battery-free devices communicate by backscattering ambient TV transmissions. The state-of-the-art ambient backscatter system [24] achieves communication rates of up to 10 kbps at distances of less than two feet. As described in §4, our design can overcome the design limitation of [24] and achieve significantly higher ranges. To demonstrate this, we first evaluate the bit error rate (BER) as a function of distance for various transmitter data rates. We then evaluate the effects of antenna separation on the observed BER values.

8.1.1 BER versus Distance

We evaluate the bit error rate (BER) as a function of the distance between the two ambient backscatter devices.

Experiments. We perform the experiments using TV transmissions in the 539 MHz range. We use a single-antenna transmitter and our two-antenna receiver placed at different distances from each other. The two antennas at the receiver are separated by half a wavelength. We compute the bit error rate (BER) observed at the receiver as a function of the distance between the transmitter and the receiver. For each distance value, we repeat the experiments at ten different adjacent positions to account for multipath effects. We compute the average BER at each distance by averaging the BER across the ten locations. Since we are interested in demonstrating high rates, we use only our 1 MHz analog bandwidth prototype. We repeat the experiments for each of four different transmission rates: 1Mbps, 100 kbps, and 10 kbps. To quantify the effect of the TV signal strength on the BER, we measure the TV power level at our backscattering transmitter using a spectrum analyzer, and collect results for four different power levels of -30 dBm, -20 dBm, -10 dBm, and 0 dBm. To compare the results with existing systems, we replicate the design in [24] at a bit rate of 10 kbps and compute the BER as a function of distance for different transmit power levels.

Results. Figs. 7(a)-(d) give BER as a function of distance between the backscattering device and receiver for each of four TV power levels. Each plot shows the results for three μmo bit rates and the 10 kbps ambient backscatter design. The plots show the following:

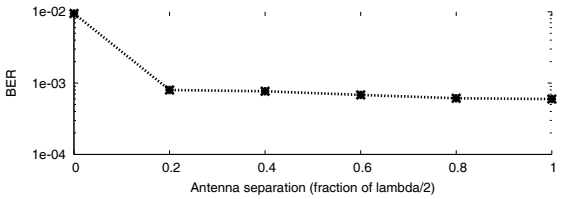

Figure 9—Effect of separation between the antennas. BER is given as a function of the antenna separation.

- The bit error rate increases as the distance between the transmitter and the receiver increases. In general, the BER increases with the bit rate. This is expected because at larger distances and higher transmission rates, noise starts affecting decodability. However, the BER values we measure for the μmo system are significantly lower than in prior work on ambient backscatter.
- As the TV power at the transmitter is reduced, the BER values across all the bit rates increase. This is because, at lower TV signal strengths, the backscatter signal power significantly reduces, decreasing the signal-to-noise ratio at the receiver. However, the BER values measured for μmo are less than 10^{-2} for distances up to 7 feet; this is true for all tested bit rates provided the TV power is greater than -20 dBm.
- At an operational BER of 10^{-2}, μmo achieves bit rates of 1 Mbps at a distance of 4 ft across the considered ambient power range. Further, when the ambient power level is greater than -20 dBm, μmo achieves 1 Mbps at distances up to 7 ft. In comparison, a 10 kbps ambient backscatter device (our baseline) can only operate at distances less than two feet across all four power levels. We note that the BER for prior single-antenna ambient backscatter designs [24] is close to 50% at 1 Mbps data rates. This is because, as explained in §4.1, prior designs leverage averaging and hence the backscattering device can transmit information only at a rate that is lower than that of averaging. Since averaging must be done over a significant time period to smooth out variations in the TV transmissions, averaging-based designs [24] do not allow rates much higher than 10 kbps. In contrast, since μmo eliminates the variations in the TV transmissions using division, it can achieve a 100X improvement in the communication rate.

8.1.2 BER Versus Antenna Separation

Next, we evaluate the effect of receive antenna separation on μmo's ability to decode backscattered transmissions. To do this, we fix the positions of the transmitter and the receiver at a distance of three feet from each other. We vary the distance between the two antennas at the receiver from half a wavelength (0.9 feet) to zero feet. The transmitter uses a bit rate of 1 Mbps and is placed in locations where the average TV power is around -10 dBm. We then compute the BER as a function of the antenna separation at the receiver. Fig. 9 plots the results of our experiments. The plot shows that as expected the BER increases as the distance between the two antennas reduces. However, the BER does not see a significant increase until the antenna separation is less than 0.2 half-wavelengths (0.18 feet). This is because while in theory a half-wavelength separation is optimal, in practice smaller receive antenna separations also have good spatial diversity due to wireless multi-path.

We also note that, even when the antenna separation is zero, the BER is still 10^{-2}. This is because, even at this minimal separation, the two antennas still experience a small phase difference that is sufficient to eliminate TV signal fluctuation and decode the backscattered signal.

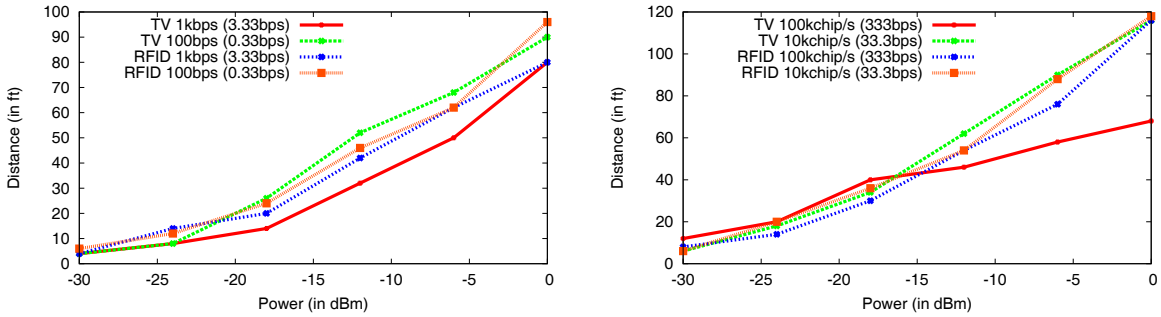

(a) With 1 kHz prototype (b) With 1 MHz prototype

Figure 8—Communication range versus power in line-of-sight scenarios. The plots show the communication range as a function of the power of the RFID and TV signals as seen by the backscattering device. We plot results for both our 1 kHz and 1 MHz prototypes.

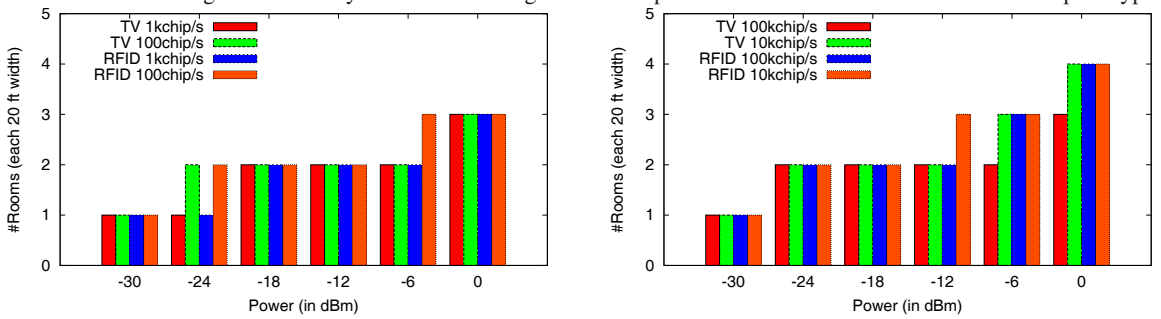

(a) With 1 kHz prototype (b) With 1 MHz prototype

Figure 10—Communication range versus power in non-line-of-sight scenarios. The receiver is moved away from the transmitter into different rooms as shown in Fig. 11. The y-axis represents the number of rooms where the BER is less than 10^{-2}.

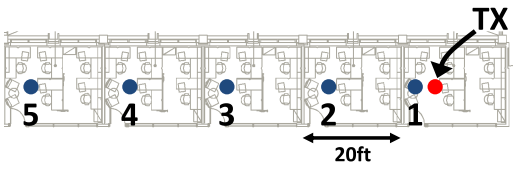

Figure 11—Non-line-of-sight experiment locations. We locate the transmitter in the middle of an office at point TX and move the receiver through several adjacent offices to determine the number of walls through which the system can continue to communicate. This is performed for both RFID tag-to-tag communication (continuous wave) and ambient backscatter (TV signal) scenarios.

8.2 Evaluating μcode

Next, we evaluate the performance of μcode in practice. As described in §5, μcode achieves two main goals. First, it enables long range RFID tag-to-tag communication by backscattering signals from an RFID reader. Second, it enables ambient backscatter communication at ranges much greater than those demonstrated by existing systems. In this section, we evaluate these goals in both line-of-sight and non-line-of-sight scenarios.

8.2.1 In Line-of-Sight Scenarios

Firstly, we evaluate μcode for RFID tag-to-tag communication and ambient backscatter in line-of-sight scenarios.

Experiments. We run experiments in a large indoor space with dimensions 120 ft $\times$ 40 ft $\times$ 60 ft. We use both the 1 MHz and 1 kHz analog bandwidth receiver prototypes that implement μcode. We pick chip rates of 100 chips/s and 1k chips/s on our 1 kHz bandwidth prototype and 10 kchips/s and 100 kchips/s on our 1 MHz bandwidth prototype. At every chip rate we use a chip length of 300 chips to represent an information bit. This combination of chip rates and chip lengths translates to bit rates of 0.33 bps, 3.33 bps, 33.3 bps, and 333 bps, respectively. We measure the range achieved by our system at different RF power levels for the RFID reader or TV signal as measured at our transmitter. To evaluate the benefits of RFID tag-to-tag communication in enable connectivity for tags far from the RFID reader, we place the transmitter (receiver) tag close to (far from) the RFID reader. We vary the power values from -30 dBm to 0 dBm by changing the position of the transmitter. For each combination of power level and transmitted bit rate, we measure the communication range between the transmitter and the receiver. To do this, we move the receiver away from the transmitter and note the distance at which the BER first goes below 10^{-2}. Note that the receiver moves away from the RFID reader in all our experiments.[3] We repeat the above experiments with TV transmissions using our TV backscatter prototypes.

Results. Fig. 8 plots communication range as a function of the signal strength of the reader and TV transmissions as measured at the transmitter. Fig. 8(a) and (b) plot the results for our 1 MHz and 1 KHz prototypes, respectively. The plots show the following:

- On each of our 1 MHz and 1 kHz prototypes, the communication range is higher at lower bit rates. This observation holds for both our TV and RFID backscatter prototypes. This is expected because higher bit rates suffer from higher noise that limits the decoding capability at longer distances.
- Our 1 MHz analog hardware generally achieves higher ranges than our 1 kHz prototype. This is expected, as the 1 MHz hardware has a higher bandwidth and hence has less effective noise.
- The communication range increases with the power of the signal at the backscattering device. Using the 1 kHz prototype, RFID tags can communicate with each other at a rate of 3.33 bps at ranges greater than 90 feet given an incident RF power of 0 dBm. At an incident power level of -15 dBm, the communica-

[3] As the receiver moves away from the reader, it can receive neither transmissions nor power from the RFID reader. Our receiver can harvest power from solar and ambient TV signals in these scenarios.

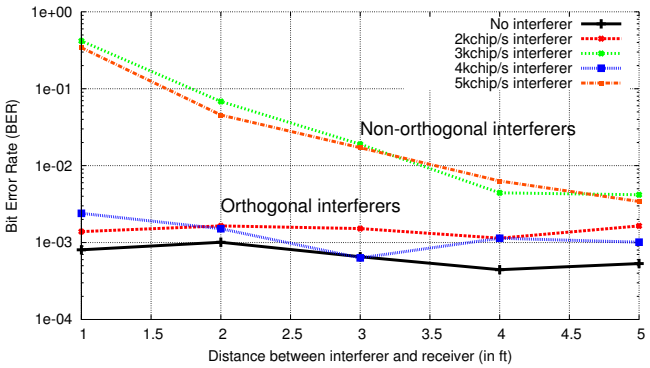

Figure 12—Multiple concurrent transmissions. We place an interferer close to a receiver configured to receive 1 kchips/s transmissions. We have the interferer transmit at 2 kchips/s and 4 kchips/s which are orthogonal codes and also at 3 kchips/s and 5 kchips/s which are non-orthogonal codes to 1 kchips/s. The plots show that the interferer increases the BER at the receiver when using non-orthogonal codes. The interference however is minimal with an interferer using orthogonal codes (2 kchips/s and 4 kchips/s).

tion range is over 30 feet with both TV and RFID transmissions. Such ranges are significantly higher than those achieved by existing systems.

8.2.2 In Non-Line-of-Sight Scenarios

Next, we evaluate μcode's performance in non-line-of-sight scenarios. Conventional RFID technology is limited to line-of-sight scenarios and is not designed to work through walls or other occluding obstacles. μcode achieves coding gains in a low-power manner that allows it to enable communication in through-the-wall scenarios. Specifically, we evaluate μcode's ability to achieve both RFID tag-to-tag communication as well as ambient backscatter communication in through-the-wall scenarios.

Experiments: We run experiments in a through-the-wall scenario in our organization, as shown in Fig. 11. The testbed spans five rooms and is separated by double sheet-rock (plus insulation) walls with a thickness of approximately 5.7 inches. Each room is about 20 feet wide and contains typical furniture one would expect in an office (e.g., chairs, tables, couches, etc.). We fix the location of our single-antenna backscattering device as shown in the testbed. We then move our receiver prototype away from the transmitter, starting at a distance of one meter with the receiver in the same room as the backscattering device (no walls), then moving the receiver to different rooms increasingly distant from the transmitter. For our RFID tag-to-tag communication results, we place the backscattering device in the presence of an RFID reader and vary the RF signal power seen at the device. To evaluate an ambient backscatter scenario, we vary the TV signal power at the backscattering device.We also run experiments with both our 1 MHz and 1 kHz receiver prototypes and with different bit rates as before. For each power level observed at the transmitter, we note the number of walls through which the receiver can still decode the backscattered signal at a BER of less than 10^{-2}.

Results. Fig. 10(a), and (b) plot the room number at which the system works, for both our 1 MHz and 1 kHz hardware. The plots show that while the devices cannot communicate through walls when the incident RF power is less than -25 dBm, through-wall communication is possible when the power level is greater than -25 dBm. This is true for both RFID tag-to-tag communication and ambient backscatter communication with TV signals. We believe this is a significant advancement in backscatter communication.

8.3 Evaluating Concurrent Transmissions with μcode

As described in §5, μcode can be used to enable concurrent transmission in the network without suffering from interference. Specifically, one can assign chip sequences that satisfy Lemma 5.2 to different transmitters, allowing them to transmit concurrently without interference. In this section, we evaluate the feasibility of achieving this in practice.

To do this, we place a transmitter and our receiver prototype at a fixed separation of 10 feet. The transmitter and receiver are configured to use a chip rate of 1 kHz and chip length of 300. We evaluate the effect of an interfering transmitter on the BER. Specifically, we place an interfering transmitter at different distances ranging from 1 feet to 5 feet away from our receiver. The interfering transmitter uses two sets of chip sequences: the first set has chip rates of 2kchips/s and 4kchips/s, and the second set has rates of 3kchips/s and 5kchips/s. The first set of chip rates are such that they satisfy the property in Lemma 5.2 and hence in theory should not interfere with the receiver. The chip rates in the second set, however, do not satisfy Lemma 5.2 and hence are expected to create interference.

Fig. 12 plots the computed BER values at the receiver as a function of distance from the interfering transmitter. The black solid line corresponds to the baseline results in the absence of an interfering transmitter. We show plots for the two sets of orthogonal (2 and 4 kchips/s) and non-orthogonal codes (3 and 5 kchips/s). The figure shows the following:

- As expected, the BER values corresponding to the non-orthogonal codes (3 and 5 kchips/s) are much higher than the baseline. Specifically, with a distance of one foot between the interference transmitter and receiver, the BER is close to 0.5 (which is similar to a random guess). The BER values improve as the distance from the interfering transmitter increases.
- The BER values for the orthogonal codes (2 and 4 kchips/s) are close to the baseline without the interfering device. This is true even when the interferer is as close as one foot away from the receiver. This demonstrates that μcode can enable concurrent transmissions without significant interference at the receivers.

9. Conclusion

We present two novel communication primitives for backscatter communication systems: μmo, a multi-antenna cancellation receiver that operates on backscatter devices, and μcode, a coding mechanism that provides the benefits of CDMA and can be decoded on backscatter devices. Using these communication primitives, we enable RFID tags to communicate directly with each other at distances of tens of meters and while separated by multiple walls. Further, we show that our designs can provide orders of magnitude increase in the communication rate and range of ambient backscatter systems. We believe that this paper represents a substantial leap forward in the capabilities of backscatter systems.

Acknowledgements. We would like to thank Ben Ransford, Vincent Liu, Rajalakshmi Nandakumar, Donny Huang, our shepherd Alex Snoeren, and the anonymous SIGCOMM reviewers for their helpful comments. This research is funded in part by UW Commercialization Gap Fund, Qualcomm Innovation Fellowship, Washington Research Foundation gift, and NSF.

10. References

[1] Minimum illumination intensities in foot-candles. https://www.osha.gov/pls/oshaweb/owadisp.show_document?p_table=STANDARDS&p_id=10630.

[2] Ieee 802.11g standard, 2003. http://standards.ieee.org/getieee802/download/802.11g-2003.pdf.

[3] Ieee 802.21 standard, 2008. http://standards.ieee.org/getieee802/download/802.21-2008.pdf.
[4] C. Boyer and S. Roy. Backscatter communication and rfid: Coding, energy, and mimo analysis. Communications, IEEE Transactions on, 2013.
[5] M. Buettner. Backscatter Protocols and Energy-Efficient Computing for RF-Powered Devices. PhD thesis, 2013.
[6] M. Buettner, B. Greenstein, and D. Wetherall. Dewdrop: an energy-aware runtime for computational rfid. In NSDI, 2011.
[7] G. M. C. Angerer, R. Langwieser and M. Rupp. Maximal ratio combining receivers for dual antenna rfid readers. In Wireless Sensing, Local Positioning, and RFID, 2009.
[8] S. Chen and T. Zhang. Low power soft-output signal detector design for wireless mimo communication systems. In ISLPED, 2007.
[9] I. Chien C, Elgorriaga and M. C. Low-power direct-sequence spread-spectrum modem architecture for distributed wireless sensor networks. In ISLPED, 2001.
[10] C. Divarathne and N. Karmakar. Mimo based chipless rfid system. In RFID-TA, 2012.
[11] J. Ghalsari and A. Ferdosi. A direct sequence spread spectrum code acquisition circuit for wireless sensor networks. In International Journal of Electronics, 2011.
[12] S. Gollakota, F. Adib, D. Katabi, and S. Seshan. Clearing the rf smog: making 802.11 n robust to cross-technology interference. In SIGCOMM, 2011.
[13] J. Griffin and G. Durgin. Gains for rf tags using multiple antennas. Antennas and Propagation, IEEE Transactions on, 2008.
[14] D. Halperin, B. Greenstein, A. Sheth, and D. Wetherall. Demystifying 802.11n power consumption. In HotPower, 2010.
[15] C. He, X. Chen, Z. Wang, and W. Su. On the performance of mimo rfid backscattering channels. EURASIP Journal on Wireless Communications and Networking, 2012.
[16] C. He and Z. Wang. Gains by a space-time-code based signaling scheme for multiple-antenna rfid tags. In CCECE, 2010.
[17] C. He and Z. J. Wang. Closed-form ber analysis of non-coherent fsk in miso double rayleigh fading/rfid channel. Communications Letters, IEEE, 2011.
[18] J. Im, M. Cho, Y. Jung, Y. Jung, and J. Kim. A low-power and low-complexity baseband processor for mimo-ofdm wlan systems. Journal of Signal Processing Systems, 2012.
[19] I. Kang and A. N. Willson Jr. Low-power viterbi decoder for cdma mobile terminals. Solid-State Circuits, IEEE Journal of, 1998.
[20] B. Kellogg, V. Talla, and S. Gollakota. Bringing gesture recognition to all devices. In NSDI, 2014.
[21] O. Koistinen, J. Lahtinen, and M. T. Hallikainen. Comparison of analog continuum correlators for remote sensing and radio astronomy. Instrumentation and Measurement, IEEE Transactions on, 2002.
[22] E. Konguvel, J. Raja, and M. Kannan. Article: A low power vlsi implementation of 2x2 mimo ofdm transceiver with ici-sc scheme. International Journal of Computer Applications, 2013.
[23] R. Langwieser, C. Angerer, and A. Scholtz. A uhf frontend for mimo applications in rfid. In RWS, 2010.
[24] V. Liu, A. Parks, V. Talla, S. Gollakota, D. Wetherall, and J. R. Smith. Ambient backscatter: wireless communication out of thin air. In SIGCOMM, 2013.
[25] T. Long and N. R. Shanbhag. Low-power cdma multiuser receiver architectures. In SiPS, 1999.
[26] A. McCormick, P. Grant, J. Thompson, T. Arslan, and A. Erdogan. Low power receiver architectures for multi-carrier cdma. IEE Proceedings-Circuits, Devices and Systems, 2002.
[27] C. Mutti and C. Floerkemeier. Cdma-based rfid systems in dense scenarios: Concepts and challenges. In RFID, 2008.
[28] P. V. Nikitin, S. Ramamurthy, R. Martinez, and K. Rao. Passive tag-to-tag communication. In RFID, 2012.
[29] Y. Okunev, K. J. Powell, M. Arneson, and W. R. Bandy. System integration of rfid and mimo technologies. US Patent App. 11/294,464.
[30] S. Padin. A wideband analog continuum correlator for radio astronomy. Instrumentation and Measurement, IEEE Transactions on, 1994.
[31] S. Padin, J. K. Cartwright, M. C. Shepherd, J. K. Yamasaki, and W. L. Holzapfel. A wideband analog correlator for microwave background observations. Instrumentation and Measurement, IEEE Transactions on, 2001.
[32] R. Piechocki, J. Garrido, D. McNamara, J. McGeehan, and A. Nix. Analog mimo detector: the concept and initial results. In International Symposium on Wireless Communication Systems, 2004.
[33] Solar-Garrido, J. Picchocki, and D. McNamara. Analog mimo detection on the basis of belief propagation. In MWSCAS, 2006.
[34] T. Takahashi, A. T. Erdogan, T. Arslan, and J. Han. Low power layered space-time channel detector architecture for mimo systems. In Emerging VLSI Technologies and Architectures, 2006.
[35] K. Terasaki, K. Kinami, and N. Honma. Passive mimo transmission using load modulation. In ISAP, 2012.
[36] D. Tse and P. Viswanath. Fundamentals of wireless communication. Cambridge university press, 2005.
[37] J. Wang, H. Hassanieh, D. Katabi, and P. Indyk. Efficient and reliable low-power backscatter networks. In SIGCOMM, 2012.
[38] L. Wang and N. Shanbhag. Low-power mimo signal processing. VLSI Systems, IEEE Transactions on, 2003.
[39] L.-C. Wuu, Y.-J. Chen, C.-H. Hung, and W.-C. Kuo. Zero-collision rfid tags identification based on cdma. In International Conference on Information Assurance and Security, 2009.
[40] Q. Yang, X. Li, H. Yao, J. Fang, K. Tan, W. Hu, J. Zhang, and Y. Zhang. Bigstation: enabling scalable real-time signal processingin large mu-mimo systems. In SIGCOMM, 2013.
[41] P. Zhang and D. Ganesan. Enabling bit-by-bit backscatter communication in severe energy harvesting environments. In NSDI, 2014.

APPENDIX

A. Proof of Lemma 5.1 Say $2T$ is the duration of a chip and the amplitudes corresponding to the one and zero bits are A_1 and A_2. For simplicity let us assume that $A_1 > A_2$. Now say that chip sequence used to compute the in-phase component I is s seconds out of synchronization from the transmitted signal. Given these parameters we can write the following:

$$\begin{aligned} I &= -sA_1 + (2T-s)A_1 + sA_2 - (2T-s)A_2 \\ &= (2T-2s)(A_1 - A_2) \end{aligned}$$

Now if $0 < s < T$, then the quadrature component Q component over one two chips (01 sequence) is

$$\begin{aligned} Q &= -(T+s)A_1 + (T+s)A_1 + (T+s)A_2 - (T-s)A_2 \\ &= -2s(A_1 - A_2) \end{aligned}$$

Thus, $|I| + |Q| = 2T(A_1 - A_2)$. On the other hand, if $T < s < 2T$, then the quadrature component Q is

$$\begin{aligned} Q &= (s-T)A_1 - (3T-s)A_1 - (s-T)A_2 + (3T-s)A_2 \\ &= (2s-4T)(A_1 - A_2) \end{aligned}$$

In this case, again, $|I| + |Q| = 2T(A_1 - A_2)$. Therefore, for any s, $|I| + |Q| = t(A_1 - A_2)$. Furthermore, for $2N$ chips, the computation result will be $NT(A_1 - A_2)$, independent of synchronization. Finally, if $A_1 = 1$, $A_2 = 0$ and $T = 1/2$, then $|I| + |Q| = N$.

B. Proof of Lemma 5.2 Our goal is to prove that a chip sequence with a code rate R is orthogonal to one with a code rate $2NR$ and of chip length $2N$. First, within the time period of one chip with a chip rate C, there are N complete alternating zero-one chips corresponding to the chip sequence with a chip rate $2NC$, independent of synchronization. Assuming that A_1 and A_2 are the amplitudes for bits one and zero, the computation for the 1 chip outputs $N(A_1 - A_2)$ or $-N(A_1 - A_2)$, and $-N(A_1 - A_2)$ or $N(A_1 - A_2)$ for 0 chip. Thus resulting in a sum of 0 when computed over two consecutive chips Similarly, the computation on the Q path will output 0 as well for two consecutive chips. Thus, $|I| + |Q| = 0$ holds for a decoder tuned to chip rate C. Next, we look at the decoder for the chip sequence at rate $2NC$ and length $2N$. Within the time period of $2N$ chips at a rate of $2NC$, there is one complete 01 chip sequence corresponding to the chip rate of C, thus the correlation computation of I and Q are zero. Thus again $|I| + |Q| = 0$, proving our lemma.